

# Nucleosynthesis in Core-Collapse Supernovae and GRB–Metal-Poor Star Connection

K. Nomoto\*, N. Tominaga\*, M. Tanaka\*, K. Maeda<sup>†</sup> and H. Umeda\*

\**Department of Astronomy, University of Tokyo, Bunkyo-ku, Tokyo 113-0033, Japan*

<sup>†</sup>*Max-Planck-Institut für Astrophysik, 85741 Garching, Germany*

## Abstract.

We review the nucleosynthesis yields of core-collapse supernovae (SNe) for various stellar masses, explosion energies, and metallicities. Comparison with the abundance patterns of metal-poor stars provides excellent opportunities to test the explosion models and their nucleosynthesis. We show that the abundance patterns of extremely metal-poor (EMP) stars, e.g., the excess of C, Co, Zn relative to Fe, are in better agreement with the yields of hyper-energetic explosions (Hypernovae, HNe) rather than normal supernovae.

We note that the variation of the abundance patterns of EMP stars are related to the diversity of the Supernova-GRB connection. We summarize the diverse properties of (1) GRB-SNe, (2) Non-GRB HNe/SNe, (3) XRF-SN, and (4) Non-SN GRB. In particular, the Non-SN GRBs (dark hypernovae) have been predicted in order to explain the origin of C-rich EMP stars. We show that these variations and the connection can be modeled in a unified manner with the explosions induced by relativistic jets. Finally, we examine whether the most luminous supernova 2006gy can be consistently explained with the pair-instability supernova model.

**Keywords:** gamma rays: bursts — nuclear reactions, nucleosynthesis, abundances — stars: abundances — stars: Population II — supernovae: general

**PACS:** 26.20.+f, 26.30.+k, 26.50.+x, 97.10.Tk, 97.60.Bw

To appear in "Supernova 1987A: 20 Years After: Supernovae and Gamma-Ray Bursters", eds. S. Immler, K. Weiler, & R. McCray (American Institute of Physics) (2007)

## INTRODUCTION

Massive stars in the range of 8 to  $\sim 130M_{\odot}$  undergo core-collapse at the end of their evolution and become Type II and Ib/c supernovae (SNe) unless the entire star collapses into a black hole with no mass ejection [e.g., 4, 33, 23].

The explosion energies of core-collapse supernovae are fundamentally important quantities, and an estimate of  $E \sim 1 \times 10^{51}$  ergs has often been used in calculating nucleosynthesis and the impact on the interstellar medium. (In the present paper, we use the explosion energy  $E$  for the final kinetic energy of explosion, and  $E_{51} = E/10^{51}$  erg.) A good example is SN1987A in the Large Magellanic Cloud, whose energy is estimated to be  $E_{51} = 1.0 - 1.5$  from its early light curve [e.g., 4, 55].

One of the most interesting recent developments in the study of supernovae is the discovery of some very energetic supernovae, whose kinetic energy (KE) exceeds  $10^{52}$  erg, more than 10 times the KE of normal core-collapse SNe. The most luminous and powerful of these objects, the Type Ic supernova (SN Ic) 1998bw, was linked to the gamma-ray

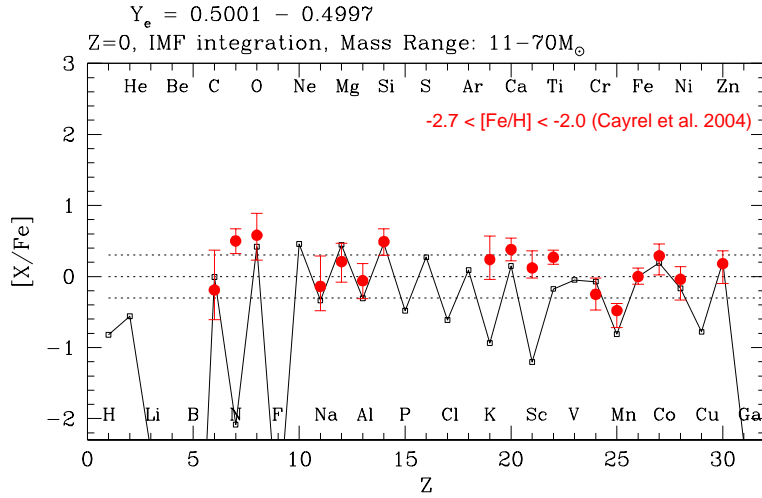


**FIGURE 1.** Comparison between the abundance pattern of VMP stars [11] (*filled circles with error bars*) and the IMF integrated yield of Pop III SNe from  $10M_\odot$  to  $50M_\odot$  [75]

burst GRB 980425 [25], thus establishing for the first time a connection between long-duration gamma-ray bursts (GRBs) and the well-studied phenomenon of core-collapse SNe [83]. However, SN 1998bw was exceptional for a SN Ic: it was as luminous at peak as a SN Ia, indicating that it synthesized  $\sim 0.5M_\odot$  of  $^{56}\text{Ni}$ , and its KE was estimated at  $E_{51} \sim 30$  [35].

In the present paper, we use the term ‘Hypernova (HN)’ to describe such a hyper-energetic supernova with  $E \gtrsim 10^{52}$  ergs without specifying the explosion mechanism [57]. Following SN 1998bw, other ‘hypernovae’ of Type Ic have been discovered or recognized [59].

Nucleosynthesis features in such hyper-energetic (and hyper-aspherical) supernovae must show some important differences from normal supernova explosions. This might be related to the unpredicted abundance patterns observed in the extremely metal-poor (EMP) halo stars [e.g., 32, 6]. This approach leads to identifying the First Stars in the Universe, i.e., metal-free, Population III (Pop III) stars which were born in a primordial hydrogen-helium gas cloud. This is one of the important challenges of the current astronomy.

## ABUNDANCE PATTERS OF METAL-POOR STARS

We have calculated the nucleosynthesis yields for various stellar masses, explosion energies, and metallicities [61, 39, 75]. From the light curve and spectra fitting of individual supernova, the relations between the mass of the progenitor, explosion energy, and produced  $^{56}\text{Ni}$  mass have been obtained.

The enrichment by a single SN can dominate the preexisting metal contents in the early universe. Therefore, the comparison between the SN model and the abundance patterns of EMP stars can provide a new way to find out the individual SN nucleosynthesis.

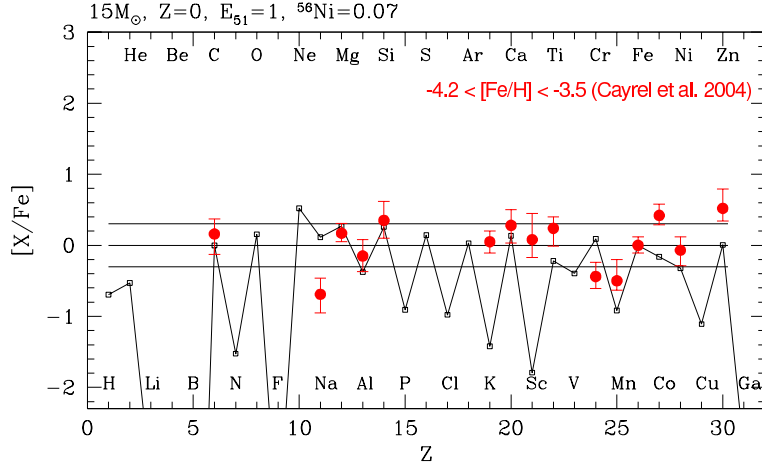


**FIGURE 2.** Averaged elemental abundances of stars with  $[\text{Fe}/\text{H}] = -3.7$  [11] compared with the normal SN yield ( $15 M_{\odot}$ ,  $E_{51} = 1$ ).

### *Very Metal-Poor (VMP) Stars*

VMP stars defined as  $[\text{Fe}/\text{H}] \lesssim -2.5$  [6] are likely to have the abundance pattern of well-mixed ejecta of many SNe. We thus compare the abundance patterns of VMP stars with the SN yields integrated over the progenitors of  $10 - 50 M_{\odot}$  (Fig. 1).

Since the abundance patterns of supernova models with  $[\text{Fe}/\text{H}] \lesssim -2.5$  are quite similar to those of Pop III star models [77, 82], we use the Pop III yields for VMP and EMP stars. Comparison between the integrated yields over the Salpeter's IMF and the abundance pattern of VMP stars (Fig. 1) show that many elements are in reasonable agreements (see [61] for further details).

### *Extremely Metal-Poor (EMP) Stars*

In the early galactic epoch when the galaxy was not yet chemically well-mixed, each EMP star ( $[\text{Fe}/\text{H}] \lesssim -2.5$ ) may be formed mainly from the ejecta of a single Pop III SN (although some of them might be the second or later generation SNe) [e.g., 2, 76]. The formation of EMP stars was driven by a supernova shock, so that  $[\text{Fe}/\text{H}]$  was determined by the ejected Fe mass and the amount of circumstellar hydrogen swept-up by the shock wave. Then, hypernovae with larger  $E$  are likely to induce the formation of stars with smaller  $[\text{Fe}/\text{H}]$ , because the mass of interstellar hydrogen swept up by a hypernova is roughly proportional to  $E$  [71] and the ratio of the ejected iron mass to  $E$  is smaller for hypernovae than for normal supernovae.

The theoretical yields are compared with the averaged abundance pattern of four EMP stars, CS 22189-009, CD-38:245, CS 22172-002 and CS 22885-096, which have low metallicity ( $-4.2 < [\text{Fe}/\text{H}] < -3.5$ ) and normal  $[\text{C}/\text{Fe}] \sim 0$  [11].

Figures 2 and 3 show that the averaged abundances of EMP stars can be fitted well with the hypernova model of  $20 M_{\odot}$  and  $E_{51} = 10$  (Fig. 3) but not with the normal SN

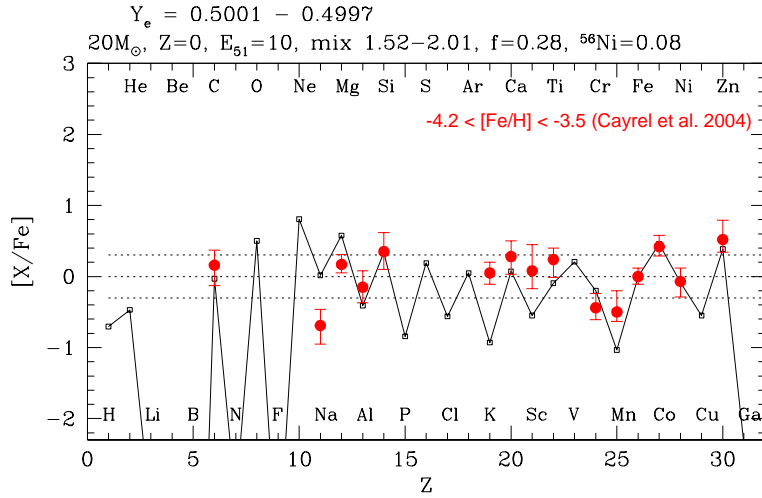


**FIGURE 3.** Averaged elemental abundances of stars with  $[\text{Fe}/\text{H}] = -3.7$  [11] compared with the hypernova yield ( $20 M_{\odot}$ ,  $E_{51} = 10$ ).

model of  $15 M_{\odot}$  and  $E_{51} = 1$  (Fig. 2) [60, 75].

In the normal SN model (Fig. 2), the mass-cut is determined to eject Fe of mass  $0.14 M_{\odot}$ . Then the yields are in reasonable agreements with the observations for  $[(\text{Na}, \text{Mg}, \text{Si})/\text{Fe}]$ , but give too small  $[(\text{Mn}, \text{Co}, \text{Ni}, \text{Zn})/\text{Fe}]$  and too large  $[(\text{Ca}, \text{Cr})/\text{Fe}]$ .

In the HN model (Fig. 3), these ratios are in much better agreement with observations. The ratios of  $\text{Co}/\text{Fe}$  and  $\text{Zn}/\text{Fe}$  are larger in higher energy explosions since both Co and Zn are synthesized in complete Si burning at high temperature region (see the next subsection). To account for the observations, materials synthesized in a deeper complete Si-burning region should be ejected, but the amount of Fe should be small. This is realized in the mixing-fallback models [78, 79].

## SUPERNOVA–GAMMA-RAY BURST CONNECTION

We have shown that nucleosynthesis in HNe is in better agreement with the abundance pattern of EMP stars. Thus it would be useful to examine the GRB-SN connection in relation to the GRB-First Star connection.

GRBs at sufficiently close distances ( $z < 0.2$ ) have been found to be accompanied by luminous core-collapse SNe Ic (GRB 980425/SN 1998bw [25]; GRB 030329/SN 2003dh [68, 34]; GRB 031203/SN 2003lw [43]). Such GRB-SN connection is now revealing quite a large diversity as follows.

(1) GRB-SNe: The three SNe Ic associated with the above GRBs have similar properties; showing broader lines than normal SNe Ic (Fig. 4: so-called broad-lined SNe [83, 50]). These three GRB-SNe have been all found to be Hypernovae (HNe), i.e., very energetic supernovae, whose *isotropic* kinetic energy (KE) exceeds  $10^{52}$  erg, about 10 times the KE of normal core-collapse SNe [35, 57, 59].

(2) Non-GRB HNe/SNe: These SNe show broad line features but are not associated with GRBs (SN 1997ef [36]; SN 2002ap [44]; SN 2003jd [45]). These are either less

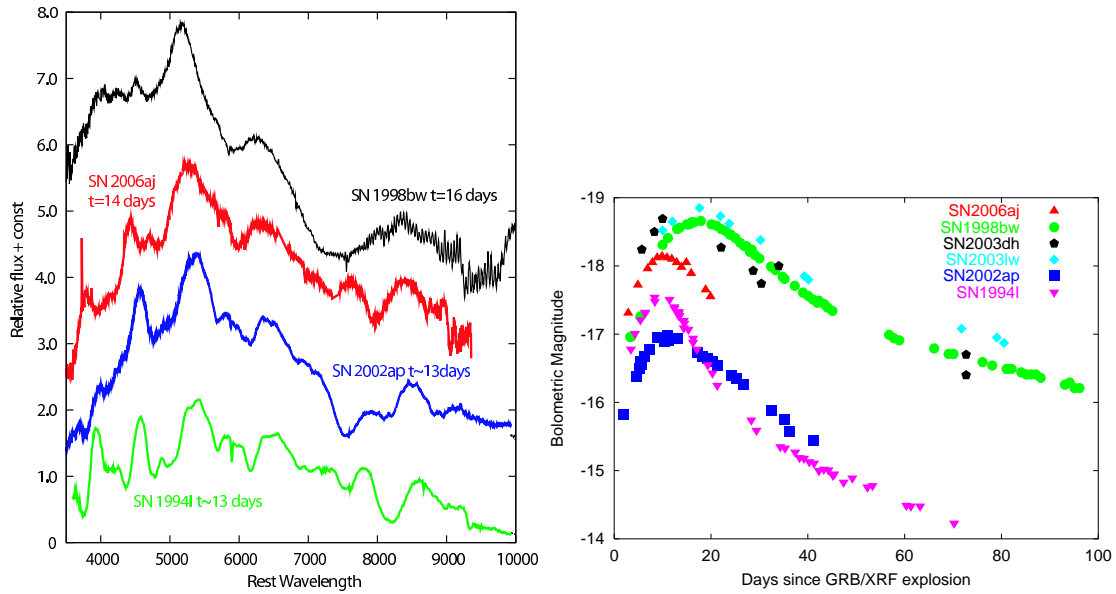


**FIGURE 4.** (Left) The spectra of 3 Hypernovae and 1 normal SN a few days before maximum. SN 1998bw/GRB 980425 represents the GRB-SNe. SN 2002ap is a non-GRB Hypernova. SN 2006aj is associated with XRF 060218, being similar to SN 2002ap. SN 1994I represents normal SNe. (Right) The bolometric light curves of GRB-SN (SNe 1998bw, 2003dh), non-GRB-SN (2002ap), XRF-SN (2006aj), and normal SNe Ic (1994I) are compared.

energetic than GRB-SNe, or observed off-axis.

(3) XRF-SNe: X-Ray Flash (XRF) 060218 has been found to be connected to SN Ic 2006aj [10, 64, 67]. The progenitor’s mass is estimated to be small enough to form a “neutron star-making SN” [47].

(4) Non-SN GRBs: We have pointed out that nucleosynthesis in HNe can explain some of the peculiar abundance patterns (such as the large Zn/Fe and Co/Fe ratios) in extremely metal-poor stars, which have long been mysteries. In particular, we have predicted that the “dark HN” (= “non-SN GRB” = long GRB with no SN) should exist and be responsible for the formation of the carbon-rich extremely (and hyper) metal-poor stars [62]. The predicted “non-SN GRBs” have been actually discovered (GRB 060605 and 060614) [18, 26, 13, 27].

### *GRB-Supernova*

Figure 4 compares the spectra of GRB-HNe (SN 1998bw), non-GRB SN, XRF-SNe, and normal SN Ic. The spectrum of SN 1998bw has very broad lines. The strongest absorptions are Ti II-Fe II (shortwards of  $\sim 4000\text{\AA}$ ), Fe II-Fe III (near  $4500\text{\AA}$ ), Si II (near  $5700\text{\AA}$ ), and O I-Ca II (between  $7000$  and  $8000\text{\AA}$ ). We calculate the synthetic spectra for ejecta models of bare C+O stars with various ejected mass  $M_{ej}$  and  $E$ . The large  $E/M_{ej}$  is required to reproduce the broad features.

The spectroscopic modelings are combined with the light curve (LC) modeling to

give the estimates of  $M_{\text{ej}}$  and  $E$ . The timescale of the LC around maximum brightness reflects the timescale for optical photons to diffuse [3]. For larger  $M_{\text{ej}}$  and smaller  $E$ , the LC peaks later and the LC width becomes broader because it is more difficult for photons to escape.

From the synthetic spectra and light curves, it was interpreted as the explosion of a massive star, with  $E_{51} \sim 30$  and  $M_{\text{ej}} \sim 10M_{\odot}$  [35]. Also the very high luminosity of SN 1998bw indicates that a large amount of  $^{56}\text{Ni}$  ( $\sim 0.5M_{\odot}$ ) was synthesized in the explosion.

The ejected  $^{56}\text{Ni}$  mass is estimated to be  $M(^{56}\text{Ni}) \sim 0.3 - 0.7M_{\odot}$  (e.g., [46]) which is 4 to 10 times larger than typical SNe Ic ( $M(^{56}\text{Ni}) \sim 0.07M_{\odot}$  [54]).

The other two GRB-SNe, 2003dh and 2003lw, are also characterized by the very broad line features and the very high luminosity.  $M_{\text{ej}}$  and  $E$  are estimated from synthetic spectra and light curves and summarized in Figure 7 [53, 15, 46]. It is clearly seen that GRB-SNe are the explosions of massive progenitor stars (with the main sequence mass of  $M_{\text{ms}} \sim 35 - 50M_{\odot}$ ), have large explosion kinetic energies ( $E_{51} \sim 30 - 50$ ), synthesized large amounts of  $^{56}\text{Ni}$  ( $\sim 0.3 - 0.5M_{\odot}$ ).

These GRB-associated HNe (GRB-HNe) are suggested to be the outcome of very energetic black hole (BH) forming explosions of massive stars (e.g., [35]).

### *Non-GRB Hypernovae*

These HNe show spectral features similar to those of GRB-SNe but are not known to have been accompanied by a GRB. The estimated  $M_{\text{ej}}$  and  $E$ , obtained from synthetic light curves and spectra, show that there is a tendency for non-GRB HNe to have smaller  $M_{\text{ej}}$  and  $E$ , and lower luminosities as summarized in Figures 7 and 8.

SN 1997ef is found to be the HN class of energetic explosion, although  $E/M_{\text{ej}}$  is a factor 3 smaller than GRB-SNe. It is not clear whether SN 1997ef is not associated with GRB because of this smaller  $E/M_{\text{ej}}$  or it was actually associated with the candidate GRB 971115.

SN 2002ap was not associated a GRB and no radio has been observed. It has similar spectral features, but narrower and redder (Fig. 4), which was modeled as a smaller energy explosion, with  $E_{51} \sim 4$  and  $M_{\text{ej}} \sim 3M_{\odot}$  [44].

The early time spectrum of SN 2003jd is similar to SN 2002ap. Interestingly, its nebular spectrum shows a double peak in O-emission lines [45]. This has exactly confirmed the theoretical prediction by the asymmetric explosion model [41]. In this case, the orientation effect might cause the non-detection of a GRB.

### *XRF-Supernovae*

GRB060218 is the second closest event as ever ( $\sim 140\text{Mpc}$ ). The GRB was weak [10] and classified as X-Ray Flash (XRF) because of its soft spectrum. The presence of SN 2006aj was soon confirmed [64, 49]. Here we summarize the properties of SN 2006aj by comparing with other SNe Ic.

SN 2006aj has several features that make it unique. It is less bright than the other GRB/SNe (Fig. 4). Its rapid photometric evolution is very similar to that of a dimmer, non-GRB SN 2002ap[44], but it is somewhat faster. Although its spectrum is characterized by broader absorption lines as in SN 1998bw and other GRB/SN, they are not as broad as those of SN 1998bw, and it is much more similar to that of SN 2002ap (Fig. 4). The most interesting property of SN 2006aj is surprisingly weak oxygen lines, much weaker than in Type Ic SNe.

By modeling the spectra and the light curve, we derive for SN 2006aj  $M_{\text{ej}} \sim 2M_{\odot}$  and  $E_{51} \sim 2$ . Lack of oxygen in the spectra indicates  $\sim 1.3M_{\odot}$  of O, and oxygen is still the dominant element. We synthesize the theoretical light curve and find that the best match is achieved with a total  $^{56}\text{Ni}$  mass of  $0.21M_{\odot}$  in which  $0.02M_{\odot}$  is located above  $20,000\text{km s}^{-1}$  (Fig. 4).

The properties of SN 2006aj (smaller  $E$  and smaller  $M_{\text{ej}}$ ) suggest that SN 2006aj is not the same type of event as the other GRB-SNe known thus far. One possibility is that the initial mass of the progenitor star is much smaller than the other GRB-SNe, so that the collapse/explosion generated less energy. If  $M_{\text{ms}}$  is  $\sim 20 - 25M_{\odot}$ , the star would be at the boundary between collapse to a black hole or to a neutron star. In this mass range, there are indications of a spread in both  $E$  and the mass of  $^{56}\text{Ni}$  synthesized[29]. The fact that a relatively large amount of  $^{56}\text{Ni}$  is required in SN 2006aj possibly suggests that the star collapsed only to a neutron star because more core material would be available to synthesize  $^{56}\text{Ni}$  in the case.

Although the kinetic energy of  $E_{51} \sim 2$  is larger than the canonical value ( $1 \times 10^{51}$  erg, [54]) in the mass range of  $M_{\text{ms}} \sim 20 - 25M_{\odot}$ , such an energy might be obtained from magnetar-type activity.

XRFs may be associated with less massive progenitor stars than those of canonical GRBs, and that the two groups may be differentiated by the formation of a neutron star[52] or a BH. In order for the progenitor star to have been thoroughly stripped of its H and He envelopes, the progenitor may be in a binary system.

### *Non-SN Gamma-Ray Bursts*

For recently discovered nearby long-duration GRB 060505 ( $z = 0.089$ , [18]) and GRB 060614 ( $z = 0.125$ , [26, 18, 13, 27]), no SN has been detected. Upper limits to brightness of the possible SNe are about 100 times fainter than SN 1998bw. These correspond to upper limits to the ejected  $^{56}\text{Ni}$  mass of  $M(^{56}\text{Ni}) \sim 10^{-3}M_{\odot}$ .

Tominaga et al. [74] calculated the jet-induced explosions (e.g., [42, 51]) of the  $40M_{\odot}$  stars [79, 75] by injecting the jets at a radius  $R \sim 900$  km, corresponding to an enclosed mass of  $M \sim 1.4M_{\odot}$ . They investigated the dependence of nucleosynthesis outcome on  $\dot{E}_{\text{dep}}$  for a range of  $\dot{E}_{\text{dep},51} \equiv \dot{E}_{\text{dep}}/10^{51}\text{ergs s}^{-1} = 0.3 - 1500$ . The diversity of  $\dot{E}_{\text{dep}}$  is consistent with the wide range of the observed isotropic equivalent  $\gamma$ -ray energies and timescales of GRBs ([1] and references therein). Variations of activities of the central engines, possibly corresponding to different rotational velocities or magnetic fields, may well produce the variation of  $\dot{E}_{\text{dep}}$ .

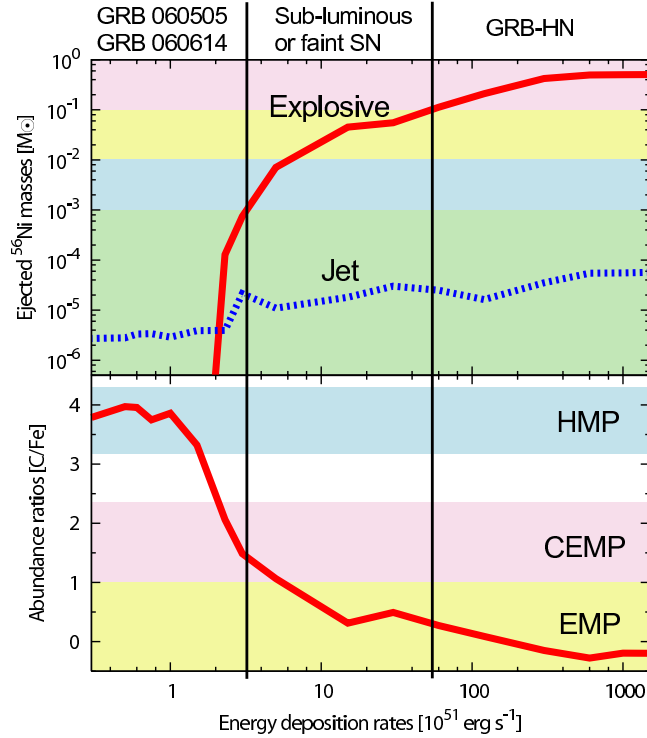


**FIGURE 5.** *Top:* the ejected  $^{56}\text{Ni}$  mass (*red:* explosive nucleosynthesis products, *blue:* the jet contribution) as a function of the energy deposition rate. The background color shows the corresponding SNe (*red:* GRB-HNe, *yellow:* sub-luminous SNe, *blue:* faint SNe, *green:* GRBs 060505 and 060614). Vertical lines divide the resulting SNe according to their brightness. *Bottom:* the dependence of abundance ratio  $[\text{C}/\text{Fe}]$  on the energy deposition rate. The background color shows the corresponding metal-poor stars (*yellow:* EMP, *red:* CEMP, *blue:* HMP stars).

## NUCLEOSYNTHESIS IN JET-INDUCED EXPLOSIONS

Nucleosynthetic properties found in the above diversity are connected to the variation of the abundance patterns of extremely-metal-poor stars, such as the excess of C, Co, Zn relative to Fe. Such a connection are modeled in a unified manner with the jet-induced explosion model.

We have computed hydrodynamics and nucleosynthesis for the explosions induced by relativistic jets. We have shown that (1) the explosions with large energy deposition rate,  $\dot{E}_{\text{dep}}$ , are observed as GRB-HNe and their yields can explain the abundances of normal EMP stars, and (2) the explosions with small  $\dot{E}_{\text{dep}}$  are observed as GRBs without bright SNe and can be responsible for the formation of the CEMP and the HMP stars. We thus propose that GRB-HNe and GRBs without bright SNe belong to a continuous series of BH-forming massive stellar deaths with the relativistic jets of different  $\dot{E}_{\text{dep}}$ .

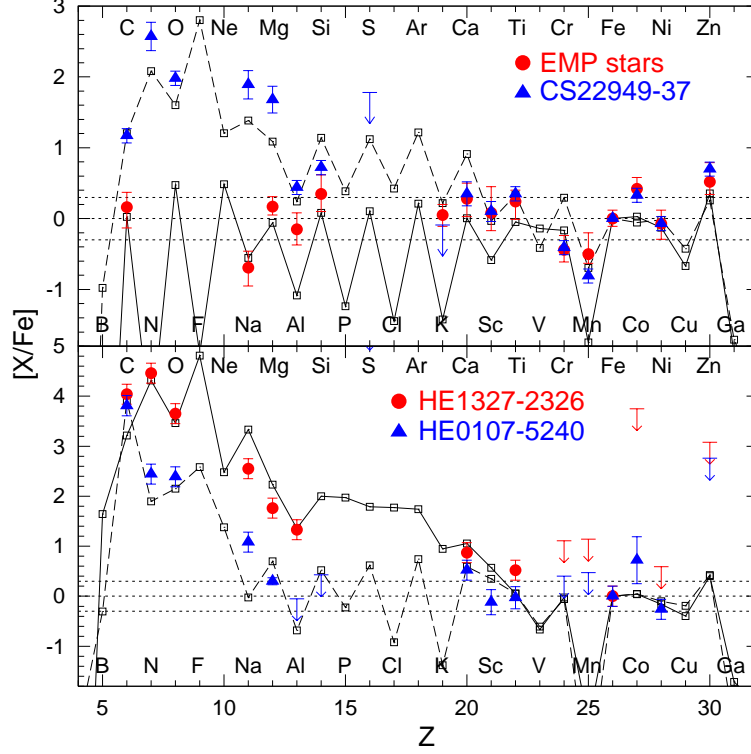


**FIGURE 6.** A comparison of the abundance patterns of metal-poor stars and of our models. *Top:* typical EMP (red dots, [11]) and CEMP (blue triangles, CS 22949–37, [16]) stars and models with  $\dot{E}_{\text{dep},51} = 120$  (solid line) and  $= 3.0$  (dashed line). *Bottom:* HMP stars: HE 1327–2326, (red dots, e.g., [20]), and HE 0107–5240, (blue triangles, [12, 8]) and models with  $\dot{E}_{\text{dep},51} = 1.5$  (solid line) and  $= 0.5$  (dashed line).

### Diversity of $^{56}\text{Ni}$ Mass

The top panel of Figure 5 shows the dependence of the ejected  $M(^{56}\text{Ni})$  on the energy deposition rate  $\dot{E}_{\text{dep}}$ . For lower  $\dot{E}_{\text{dep}}$ , smaller  $M(^{56}\text{Ni})$  is synthesized in explosive nucleosynthesis because of lower post-shock densities and temperatures (e.g., [42, 51]).

If  $\dot{E}_{\text{dep},51} \gtrsim 3$ , the jet injection is initiated near the bottom of the C+O layer, leading to the synthesis of  $M(^{56}\text{Ni}) \gtrsim 10^{-3}M_{\odot}$ . If  $\dot{E}_{\text{dep},51} < 3$ , on the other hand, the jet injection is delayed and initiated near the surface of the C+O core; then the ejected  $^{56}\text{Ni}$  is as small as  $M(^{56}\text{Ni}) < 10^{-3}M_{\odot}$ .

$^{56}\text{Ni}$  contained in the relativistic jets is only  $M(^{56}\text{Ni}) \sim 10^{-6} - 10^{-4}M_{\odot}$  because the total mass of the jets is  $M_{\text{jet}} \sim 10^{-4}M_{\odot}$  in our model with  $\Gamma_{\text{jet}} = 100$  and  $E_{\text{dep}} = 1.5 \times 10^{52}$  ergs. Thus the  $^{56}\text{Ni}$  production in the jets dominates over explosive nucleosynthesis in the stellar mantle only for  $\dot{E}_{\text{dep},51} < 1.5$  in the present model.

For high energy deposition rates ( $\dot{E}_{\text{dep},51} \gtrsim 60$ ), the explosions synthesize large  $M(^{56}\text{Ni})$  ( $\gtrsim 0.1M_{\odot}$ ) being consistent with GRB-HNe. The remnant mass was  $M_{\text{rem}}^{\text{start}} \sim 1.5M_{\odot}$  when the jet injection was started, but it grows as material is accreted from the equatorial plane. The final BH masses range from  $M_{\text{BH}} = 10.8M_{\odot}$  for  $\dot{E}_{\text{dep},51} = 60$  to

$M_{\text{BH}} = 5.5M_{\odot}$  for  $\dot{E}_{\text{dep},51} = 1500$ , which are consistent with the observed masses of stellar-mass BHs [5]. The model with  $\dot{E}_{\text{dep},51} = 300$  synthesizes  $M(^{56}\text{Ni}) \sim 0.4M_{\odot}$  and the final mass of BH left after the explosion is  $M_{\text{BH}} = 6.4M_{\odot}$ .

For low energy deposition rates ( $\dot{E}_{\text{dep},51} < 3$ ), the ejected  $^{56}\text{Ni}$  masses ( $M(^{56}\text{Ni}) < 10^{-3}M_{\odot}$ ) are smaller than the upper limits for GRBs 060505 and 060614. The final BH mass is larger for smaller  $\dot{E}_{\text{dep}}$ . While the material ejected along the jet-direction involves those from the C+O core, the material along the equatorial plane fall back.

If the explosion is viewed from the jet direction, we would observe GRB without SN re-brightening. This may be the situation for GRBs 060505 and 060614. In particular, for  $\dot{E}_{\text{dep},51} < 1.5$ ,  $^{56}\text{Ni}$  cannot be synthesized explosively and the jet component of the Fe-peak elements dominates the total yields (Fig. 6). The models eject very little  $M(^{56}\text{Ni})$  ( $\sim 10^{-6}M_{\odot}$ ).

For intermediate energy deposition rates ( $3 \lesssim \dot{E}_{\text{dep},51} < 60$ ), the explosions eject  $10^{-3}M_{\odot} \lesssim M(^{56}\text{Ni}) < 0.1M_{\odot}$  and the final BH masses are  $10.8M_{\odot} \lesssim M_{\text{BH}} < 15.1M_{\odot}$ . The resulting SN is faint ( $M(^{56}\text{Ni}) < 0.01M_{\odot}$ ) or sub-luminous ( $0.01M_{\odot} \lesssim M(^{56}\text{Ni}) < 0.1M_{\odot}$ ).

Nearby GRBs with faint or sub-luminous SNe have not been observed. This may be because they do not occur intrinsically in our neighborhood or because the number of observed cases is still too small. In the latter case, further observations may detect GRBs with a faint or sub-luminous SN.

### *Abundance Patterns of C-rich Metal-Poor Stars*

The bottom panel of Figure 5 shows the dependence of the abundance ratio [C/Fe] on  $\dot{E}_{\text{dep}}$ . Lower  $\dot{E}_{\text{dep}}$  yields larger  $M_{\text{BH}}$  and thus larger [C/Fe], because the infall decreases the amount of inner core material (Fe) relative to that of outer material (C) (see also [42]). As in the case of  $M(^{56}\text{Ni})$ , [C/Fe] changes dramatically at  $\dot{E}_{\text{dep},51} \sim 3$ .

The abundance patterns of the EMP stars are good indicators of SN nucleosynthesis because the Galaxy was effectively unmixed at  $[\text{Fe}/\text{H}] < -3$  (e.g., [76]). They are classified into three groups according to [C/Fe]:

- (1) [C/Fe]  $\sim 0$ , normal EMP stars ( $-4 < [\text{Fe}/\text{H}] < -3$ , e.g., [11]);
- (2) [C/Fe]  $\gtrsim +1$ , Carbon-enhanced EMP (CEMP) stars ( $-4 < [\text{Fe}/\text{H}] < -3$ , e.g., CS 22949–37 [16]);
- (3) [C/Fe]  $\sim +4$ , hyper metal-poor (HMP) stars ( $[\text{Fe}/\text{H}] < -5$ , e.g., HE 0107–5240 [12, 8]; HE 1327–2326 [20]).

Figure 6 shows that the general abundance patterns of the normal EMP stars, the CEMP star CS 22949–37, and the HMP stars HE 0107–5240 and HE 1327–2326 are reproduced by models with  $\dot{E}_{\text{dep},51} = 120, 3.0, 1.5,$  and  $0.5$ , respectively. The model for the normal EMP stars ejects  $M(^{56}\text{Ni}) \sim 0.2M_{\odot}$ , i.e. a factor of 2 less than SN 1998bw. On the other hand, the models for the CEMP and the HMP stars eject  $M(^{56}\text{Ni}) \sim 8 \times 10^{-4}M_{\odot}$  and  $4 \times 10^{-6}M_{\odot}$ , respectively, which are always smaller than the upper limits for GRBs 060505 and 060614. The N/C ratio in the models for CS 22949–37 and HE 1327–2326 is enhanced by partial mixing between the He and H layers during presupernova evolution [37].

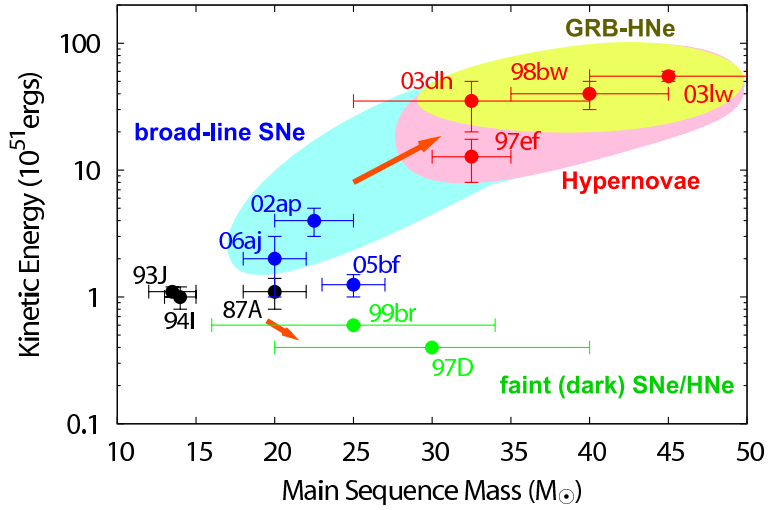


**FIGURE 7.** The kinetic explosion energy  $E$  as a function of the main sequence mass  $M$  of the progenitors for several supernovae/hypernovae. SNe that are observed to show broad-line features are indicated. Hypernovae are the SNe with  $E_{51} > 10$ .

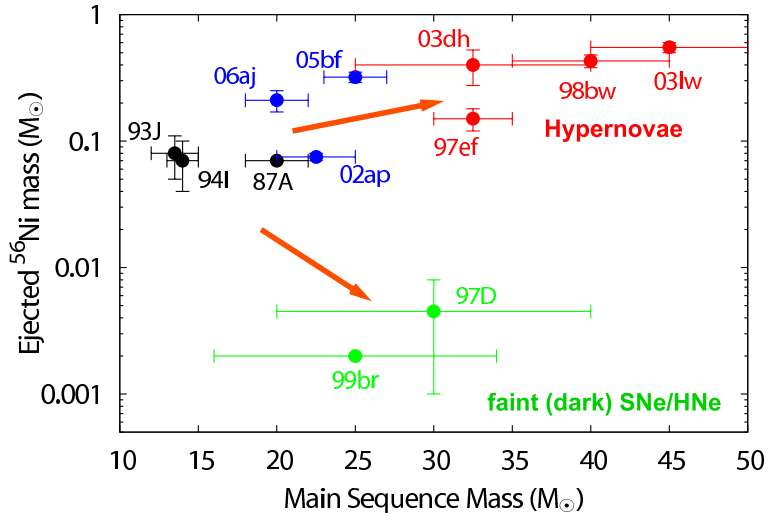


**FIGURE 8.** The ejected  $^{56}\text{Ni}$  mass as a function of the main sequence mass  $M$  of the progenitors for several supernovae/hypernovae.

## DISCUSSION

The large Zn and Co abundances and the small Mn and Cr abundances observed in very metal-poor stars can better be explained by introducing HNe. This would imply that HNe have made significant contributions to the early Galactic chemical evolution,

In theoretical models, some element ratios, such as (K, Sc, Ti, V)/Fe, are too small, while some ratios such as Cr/Fe are too large compared with the observed abundance ratios [11]. Underproduction of Sc and K may require significantly higher entropy

environment for nucleosynthesis, e.g., the “low density” progenitor models for K, Sc, and Ti [79, 24]. GRBs would have possible nucleosynthesis site, such as accretion disks around the black hole [65].

Neutrino processes in the deepest layers of SN ejecta and a possible accretion disk around a black hole would open a new window for SN nucleosynthesis [65, 21, 22, 80].

### *GRB, Hypernovae, and Broad-Lines*

Figures 7 and 8 summarize the properties of core-collapse SNe as a function of the main-sequence mass  $M_{\text{ms}}$  of the progenitor star [58]. The broad-line SNe include both GRB-SNe and Non-GRB SNe.

(1) GRB vs. Non-GRB: Three GRB-SNe are all similar Hypernovae (i.e.,  $E_{51} \gtrsim 10$ ). Thus  $E$  could be closely related to the formation of GRBs. SN 1997ef seems to be a marginal case.  $E/M_{\text{ej}}$  could be more important because SN 1997ef has significantly smaller  $E/M_{\text{ej}}$  than GRB-SNe.

(2) Broad-Line features: The mass contained at  $v > 30,000 \text{ km s}^{-1}$  (or even higher boundary velocity) might be critical in forming the broad-line features, although further modeling is required to clarify this point [61].

### *Black Holes vs. Neutron Stars*

The discovery of XRF 060218/SN 2006aj and their properties extend the GRB-HN connection to XRFs and to the HN progenitor mass as low as  $\sim 20M_{\odot}$ . The XRF 060218 may be driven by a neutron star rather than a black hole.

The final fate of 20 - 25  $M_{\odot}$  stars show interesting variety. Even normal SN Ib 2005bf is very different from previously known SNe/HNe [73, 19]. This mass range corresponds to the transition from the NS formation to the BH formation. The NSs from this mass range could be much more active than those from lower mass range because of possibly much larger NS masses (near the maximum mass) or possibly large magnetic field (*magnetar*). XRFs and GRBs from the mass range of 20 - 25  $M_{\odot}$  might form a different population.

### *Hypernovae of Type II and Type Ib?*

Suppose that smaller losses of mass and angular momentum from low metallicity massive stars lead to the formation of more rapidly rotating NSs or BHs and thus more energetic explosions. Then we predict the existence of Type Ib and Type II HNe [30].

So far all observed HNe are of Type Ic. However, most of SNe Ic are suggested to have some He [9]. If even the small amount of radioactive  $^{56}\text{Ni}$  is mixed in the He layer, the He feature should be seen [40, 56]. For HNe, the upper mass limit of He has been estimated to be  $\sim 2M_{\odot}$  [44] for the case of no He mixing. If He features would be

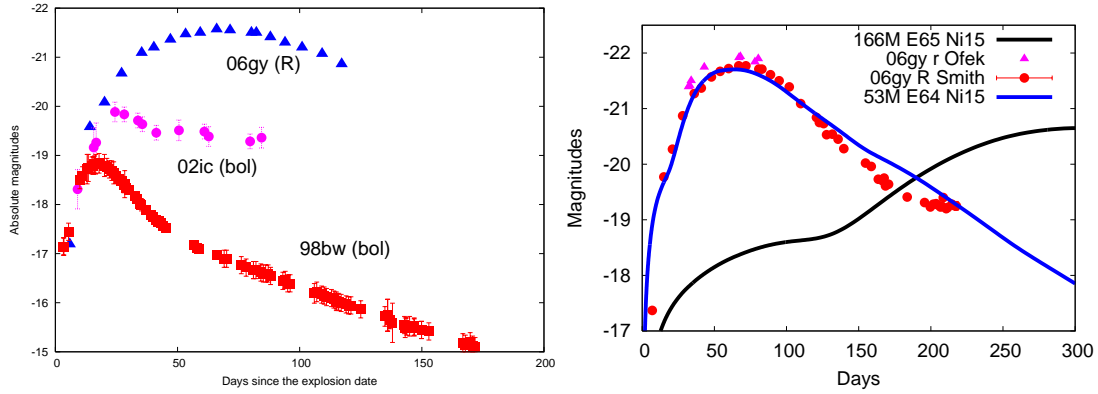


**FIGURE 9.** (Left) Comparison between LCs of SNe 1998bw (*open square* [25]), 2002ic (*open circle* [28]), and 2006gy (*filled triangle* [66]). (Right) Comparison between R- and r-band LCs of SN 2006gy [63, 66] and synthetic LCs for a model with  $M_{\text{ej}} = 53M_{\odot}$ ,  $E_{51} = 64$ , and  $M(^{56}\text{Ni}) = 15M_{\odot}$  and a PISN model with  $M_{\text{ej}} = 166M_{\odot}$ ,  $E_{51} = 65$ , and  $M(^{56}\text{Ni}) = 15M_{\odot}$ .

seen in future HN observations, it would provide an important constraint on the models, especially, the fully mixed WR models [85, 84, 48].

## MOST LUMINOUS SUPERNOVA 2006GY

Recently, several extremely luminous supernovae have been discovered, which includes SNe Iia 1997cy, 2002ic, and SN Ic 1999as (Fig. 9: left). The energy sources of these SN light curves (LC) are closely related to SN nucleosynthesis. The post-maximum light curves (LCs) of SNe Iia are powered by circumstellar interaction [14], although whether the underlying SNe are Ia or Ic is under debate [7].

SN 2006gy is the most luminous SN [63, 66]. It shows hydrogen emission features like SNe IIn and Iia to indicate circumstellar interaction. However, the X-ray luminosity is too low to explain the observed optical luminosity [66]. This suggests that the LC of SN 2006gy may be powered by the decays of  $^{56}\text{Ni} \rightarrow ^{56}\text{Co} \rightarrow ^{56}\text{Fe}$ , and the required large  $^{56}\text{Ni}$  mass,  $M(^{56}\text{Ni})$ , suggests that SN 2006gy could be a pair-instability supernova (PISN) [78, 31] rather than a core-collapse [63, 66].

We have constructed the LC model of the PISN model as shown by the solid line with 166M in Fig. 9 (right). Here we have calculated the evolution from the main-sequence with extensive mass loss to expose a C+O core. The star undergoes PISN with  $M_{\text{ej}} = 166M_{\odot}$ ,  $E_{51} = 65$ , and  $M(^{56}\text{Ni}) = 15M_{\odot}$ . Here the explosion energy is not a free parameter (like a core-collapse model) but obtained from the nuclear energy release associated with the production of  $M(^{56}\text{Ni})$ . Such a large  $M_{\text{ej}}$ , which is necessary to produce large enough  $M(^{56}\text{Ni})$ , is too large for the LC. The model LC evolves much *slower* than the observed LC of SN 2006gy (red points in Fig. 9: right).

In order to reproduce the LC of SN 2006gy, we artificially reduce the ejected mass of the above exploding model down to  $M_{\text{ej}} = 53M_{\odot}$ , keeping  $E_{51} = 64$ , and  $M(^{56}\text{Ni}) = 15M_{\odot}$  (the 53M line in Fig. 9). In other words, the progenitor should have lost much more mass than the actual model, yet produced a large enough amount of  $^{56}\text{Ni}$ .

These results imply whether SN 2006gy is a core-collapse SN or a PISN is not clear yet. The PISN model can produce enough  $M(^{56}\text{Ni})$  but  $M_{\text{ej}}$  might be too large. The core-collapse models currently available could produce too small  $M(^{56}\text{Ni})$ .

Also, the mass loss from such a massive star with solar metallicity would be too large to keep hydrogen-rich circumstellar matter as observed like SNe II<sub>n</sub> and II<sub>a</sub> [63]. Stellar merging in a close binary system or a dense star cluster might be necessary for the formation and evolution of very massive stars. Further study is clearly necessary to understand the evolutionary origin and nucleosynthesis of SN 2006gy.

## REFERENCES

1. Amati, L., Della Valle, M., Frontera, F., et al., *A&A* **463** (2007) 913
2. Argast, D., Samland, M., Gerhard, O.E., & Thielemann, F.-K., *A&A* **356** (2000) 873
3. Arnett, W. D. *ApJ* **253** (1982) 785
4. Arnett, W.D., *Supernovae and Nucleosynthesis* (Princeton Univ. Press) (1996)
5. Bailyn, C.D., Jain, R.K., Coppi, P., & Orosz, J.A., *ApJ* **499** (1998) 367
6. Beers, T., & Christlieb, N., *ARA&A* **43** (2005) 531
7. Benetti, S., et al., *ApJ* **653** (2006) L129
8. Bessell, M. S., & Christlieb, N., in *IAU Symp 228, From Lithium to Uranium*, ed. V. Hill et al. (Cambridge Univ. Press) (2005) 237
9. Branch, D., Jeffery, D.J., Timothy, R.Y., & Baron, E., *PASP* **118** (2006) 791
10. Campana, S., et al., *Nature* **442** (2006) 1008
11. Cayrel, R., et al., *A&A* **416** (2004) 1117
12. Christlieb, N., et al., *Nature* **419** (2002) 904
13. Della Valle, M., et al., 2006, *Nature* **444** (2006) 1050
14. Deng, J., Kawabata, K.S., Ohyama, Y., Nomoto, K., et al., *ApJ* **605** (2004) L37
15. Deng, J., Tominaga, N., Mazzali, P.A., Maeda, K., & Nomoto, K., *ApJ* **624** (2005) 898
16. Depagne, E., et al., *A&A* , **390** (2002) 187
17. Fynbo, J.P.U., et al., *ApJ* **609** (2004) 962
18. Fynbo, J.P.U., et al., *Nature* **444** (2006) 1047
19. Folatelli, G., et al., *ApJ* **641** (2006) 1039
20. Frebel, A., et al., *Nature* **434** (2005) 871
21. Fröhlich, C., Hauser, P., Liebendörfer, M., Martínez-Pinedo, G., Thielemann, F.-K., Bravo, E., Zinner, N. T., Hix, W. R., Langanke, K., Mezzacappa, A., & Nomoto, K., *ApJ* **637** (2006) 415
22. Fröhlich, C., Martínez-Pinedo, G., Liebendörfer, M., et al., *Phys Rev Let* **96** (2006) 142502
23. Fryer, C. L. (ed.) *Stellar Collapse* (Astrophysics and Space Science Library: Kluwer) (2004)
24. Fryer, C. L., Young, P. A., & Hungerford, A. L., *ApJ* **650** (2006) 1028
25. Galama, T., et al., *Nature* **395** (1998) 670
26. Gal-Yam, A., et al., *Nature* **444** (2006) 1053
27. Gehrels, N., et al., *Nature* **444** (2006) 1044
28. Hamuy, M., et al., *Nature* **424** (2003) 651
29. Hamuy, M., *ApJ* **582** (2003) 905
30. Hamuy, M., Contreras, C., Gonzalez, S., Krzeminski, W., *IAU Circ.* (2005) 8520
31. Heger, A., & Woosley, S.E., *ApJ* **567** (2002) 532
32. Hill, V., François, P., & Primas, F. (ed.), *IAU Symp 228, From Lithium to Uranium: Elemental Tracers of Early Cosmic Evolution* (Cambridge Univ. Press) (2005)
33. Hillebrandt, W., & Leibundgut, B. (ed.), *From Twilight to Highlight: The Physics of Supernovae* (Springer) (2003)
34. Hjorth, J., et al., *Nature* **423** (2003) 847
35. Iwamoto, K., Mazzali, P.A., Nomoto, K., et al., *Nature* **395** (1998) 672
36. Iwamoto, K., Nakamura, T., Nomoto, K., et al., *ApJ* **534** (2000) 660
37. Iwamoto, N., Umeda, H., Tominaga, N., Nomoto, K., & Maeda, K., *Science* **309** (2005) 451
38. Kawabata, K., et al., *ApJ* **580** (2002) L39

39. Kobayashi, C., Umeda, H., Nomoto, K., Tominaga, N., & Ohkubo, T., *ApJ* **653** (2006) 1145
40. Lucy, L.B., *ApJ* **383** (1991) 308
41. Maeda, K., Nakamura, T., Nomoto, K., Mazzali, P.A., Patat, F., & Hachisu, I. *ApJ* **565** (2002) 405
42. Maeda, K. & Nomoto, K., *ApJ* **598** (2003) 1163
43. Malesani, J., et al., *ApJ* **609** (2006) L5
44. Mazzali, P.A., Deng, J., Maeda, K., Nomoto, K., et al., *ApJ* **572** (2002) L61
45. Mazzali, P. A., Kawabata, K.S., Maeda, K., Nomoto, K., et al., *Science* **308** (2005) 1284
46. Mazzali, P. A., et al., *ApJ* **645** (2006a) 1323
47. Mazzali, P.A., Deng, J., Nomoto, K., et al., *Nature* **442** (2006b) 1018
48. Meynet, G., & Maeder, A., *A&A* **464** (2007) L11
49. Modjaz, M., et al. *ApJ* **645** (2006) L21
50. Modjaz, M., et al., *AJ* (2007) submitted (astro-ph/0701246)
51. Nagataki, S., Mizuta, A., & Sato, K., *ApJ* **647** (2006) 1255
52. Nakamura, T., *Prog. Theor. Phys.* **100** (1998) 921
53. Nakamura, T., Mazzali, P.A., Nomoto, K., Iwamoto, K., *ApJ* **550** (2001) 991
54. Nomoto, K., et al., *Nature* **371** (1994) 227
55. Nomoto, K., Shigeyama, T., Kumagai, S., Yamaoka, H., & Suzuki, T., in *Supernovae*, Les Houche Session LIV (1994) ed. S. Bludmann et al. (North-Holland) 489
56. Nomoto, K., Iwamoto, K., & Suzuki, T. *Phys. Rep.* **256** (1995) 173
57. Nomoto, K., Mazzali, P.A., Nakamura, T., et al., in *Supernovae and Gamma Ray Bursts*, eds. M. Livio et al. (Cambridge Univ. Press) (2001) 144 (astro-ph/0003077)
58. Nomoto, K., et al., in *IAU Symp 212, A massive Star Odyssey, from Main Sequence to Supernova*, eds. V.D. Hucht, et al. (San Francisco: ASP) (2003) 395 (astro-ph/0209064)
59. Nomoto, K., et al., in *Stellar Collapse*, ed. C.L. Fryer (Astrophysics and Space Science: Kluwer) (2004) 277 (astro-ph/0308136)
60. Nomoto, K., Tominaga, N., Umeda, H., & Kobayashi, C., in *IAU Symp 228, From Lithium to Uranium*, ed. V. Hill et al. (Cambridge Univ. Press) (2005) 287 (astro-ph/0603433)
61. Nomoto, K., Tominaga, N., Umeda, H., Kobayashi, C., & Maeda, K., *Nuclear Phys A* **777** (2006) 424 (astro-ph/0605725)
62. Nomoto, K., et al., *Nuovo Cimento* **121** (2007) 1207 (astro-ph/0702472); the ppt file available from "program" at <http://www.merate.mi.astro.it/docM/OAB/Research/SWIFT/sanservolo2006/>
63. Ofek, E.O., et al., *ApJ* **659** (2007) L13
64. Pian, E., et al., *Nature* **442** (2006) 1011
65. Pruet, J., Woosley, S.E., Buras, R., Janka, H.-T., & Hoffman, R.D., *ApJ* **623** (2005) 325
66. Smith, N., et al., *ApJ* (2007) in press (astro-ph/0612617)
67. Soderberg, A.M., et al., *Nature* **442** (2006) 1014
68. Stanek, K.Z., et al., *ApJ* **591** (2003) L17
69. Thompson, T.A., & Duncan, R.C., *Mon. Not. Royal Astron. Soc.* **275** (1995) 255
70. Thompson, T.A., Chang, P., & Quataert, E., *ApJ* **611** (2004) 380
71. Thornton, K., Gaudlitz, M., Janka, H.-Th., & Steinmetz, M., *ApJ* **500** (1998) 95
72. Tominaga, N., Deng, J., Mazzali, P.A., Maeda, K., Nomoto, K., et al., *ApJ* **612** (2004) L105
73. Tominaga, N., Tanaka, M., Nomoto, K., et al., *ApJ* **633** (2005) L97
74. Tominaga, N., Maeda, K., Umeda, H., Nomoto, K., Tanaka, et al., *ApJ* **657** (2007) L77
75. Tominaga, N., Umeda, H., & Nomoto, K., *ApJ* **660** (2007) 516
76. Tumlinson, J., *ApJ* **641** (2006) 1
77. Umeda, H., Nomoto, K., & Nakamura, T., in *The First Stars* (2000), ed. A. Weiss, T. Abel, & V. Hill (Berlin: Springer), 150 (astro-ph/9912248)
78. Umeda, H., & Nomoto, K., *ApJ* **565** (2002) 385
79. Umeda, H., & Nomoto, K., *ApJ* **619** (2005) 427
80. Wanajo, S., *ApJ* **647** (2006) 1323
81. Wang, L., Baade, D., Höflich, P., & Wheeler, J.C., *ApJ* **592** (2003) 457
82. Woosley, S. E., & Weaver, T. A., *ApJS* **101** (1995) 181
83. Woosley, S. E., & Bloom, J.S., *ARA&A* **44** (2006) 507
84. Woosley, S. E., & Heger, A., *ApJ* **637** (2006) 914
85. Yoon, S.-C., & Langer, N., *A&A* **443** (2006) 643